

A nonlinear piezoelectric mixed solid shell finite element formulation

S. Klinkel*, W. Wagner

Institut für Baustatik, Universität Karlsruhe, Kaiserstr. 12, D-76131 Karlsruhe, Germany

Abstract

This paper is concerned with a piezoelectric solid shell finite element formulation. A geometrically non-linear theory allows large deformations and includes stability problems. The finite element formulation is based on a variational principle including six independent fields: displacements, electric potential, strains, electric field, mechanical stresses and dielectric displacements. The element has 8 nodes; the nodal degrees of freedom are displacements and the electric potential. To obtain correct results in bending-dominated situations a linear distribution through the thickness of the independent electric field is assumed. The presented finite shell element is able to model arbitrary curved shell structures and incorporates a 3D-material law. As numerical example a piezoelectric buckling problem is presented.

Keywords: Solid shell finite element; Smart structures; Piezoelectricity; Electro-elasticity

1. Introduction

In this paper a piezoelectric solid shell element is developed. In recent years several new elements have been proposed. Some of these model a reference surface of the shell structure, see e.g. [1,2]. With respect to the laminated structure of piezoelectric devices a more or less sophisticated laminate theory is necessary. The so-called solid shell elements circumvent laminate theories by modelling each ply with one element, see e.g. [3].

The above cited piezoelectric shell formulations assume a geometrically linear theory. In [4] it is pointed out that nonlinear characteristics can significantly influence the performance of piezoelectric systems. In particular this holds for buckling of plates. The most nonlinear piezoelectric plate formulations e.g. [4,5] use von Karman plate theory, which represents a nonlinear theory of lowest order and does not account for all geometric nonlinearities.

Usually the electric potential inside the piezoelectric model is assumed to be linear through the shell thickness. To fulfill the electric charge conservation law exactly a quadratic electric potential through the thickness is necessary. A quadratic approximation was

introduced for shell elements in [1,2] and leads in general to an additional degree of freedom.

In this paper a mixed formulation is proposed. Recently a geometrically linear hybrid formulation was introduced in [3], where stresses, displacements, and the electric potential are considered in the variational formulation.

The essential features and novel aspects of the present element are summarized as follows:

- The mixed finite element formulation is based on a variational principle including six independent field variables, which are displacements, electric potential, strains, electric field, stresses, and dielectric displacements.
- The electric field is assumed to be linear through the shell thickness, which fulfills the electric charge conservation law in bending dominated situations exactly.
- A solid shell element with 8 nodes and 4 nodal degrees of freedom is presented. Internal degrees of freedom are eliminated by a static condensation on element level.
- A complete geometrically non-linear theory is considered. It allows large deformations and accounts for stability problems.

* Corresponding author. Tel.: +49 721 608 2280; Fax: +49 721 608 6015; E-mail: sk@bs.uni-karlsruhe.de

2. Gradient fields

In this section the Green–Lagrangean strains and the electric field are derived in convective co-ordinates. The parameter ξ^3 is defined as thickness co-ordinate and ξ^1 , ξ^2 as in-plane co-ordinates of the considered shell formulation. The position vector of the reference configuration \mathcal{B}_0 and the current configuration \mathcal{B}_t are denoted by \mathbf{X} and $\mathbf{x} = \mathbf{X} + \mathbf{u}$, where \mathbf{u} is the displacement vector. The covariant tangent vectors are defined as:

$$\mathbf{G}_i = \frac{\partial \mathbf{X}}{\partial \xi^i}, \quad \mathbf{g}_i = \frac{\partial \mathbf{x}}{\partial \xi^i}, \quad i = 1, 2, 3 \quad (1)$$

Introducing the metric coefficients $g_{ij} = \mathbf{g}_i \cdot \mathbf{g}_j$ and $G_{ij} = \mathbf{G}_i \cdot \mathbf{G}_j$ the Green–Lagrangean strain components read:

$$E_{ij} = \frac{1}{2}(g_{ij} - G_{ij}) \quad (2)$$

and are arranged in a vector $\mathbf{E}_{cova} = [E_{11}, E_{22}, E_{33}, 2E_{12}, 2E_{13}, 2E_{23}]^T$

Introducing

$T_s =$

$$\begin{bmatrix} (J_{11})^2 & (J_{12})^2 & (J_{13})^2 & 2J_{11}J_{12} & 2J_{11}J_{13} & 2J_{12}J_{13} \\ (J_{21})^2 & (J_{22})^2 & (J_{23})^2 & 2J_{21}J_{22} & 2J_{21}J_{23} & 2J_{22}J_{23} \\ (J_{31})^2 & (J_{32})^2 & (J_{33})^2 & 2J_{31}J_{32} & 2J_{31}J_{33} & 2J_{32}J_{33} \\ J_{11}J_{21} & J_{12}J_{22} & J_{13}J_{23} & J_{11}J_{22} + J_{12}J_{21} & J_{11}J_{23} + J_{13}J_{21} & J_{12}J_{23} + J_{13}J_{22} \\ J_{11}J_{31} & J_{12}J_{32} & J_{13}J_{33} & J_{11}J_{32} + J_{12}J_{31} & J_{11}J_{33} + J_{13}J_{31} & J_{12}J_{33} + J_{13}J_{32} \\ J_{21}J_{31} & J_{22}J_{32} & J_{23}J_{33} & J_{21}J_{32} + J_{22}J_{31} & J_{21}J_{33} + J_{23}J_{31} & J_{22}J_{33} + J_{23}J_{32} \end{bmatrix} \quad (3)$$

with $J_{ik} = \mathbf{t}_i \cdot \mathbf{G}_k$ and $\mathbf{t}_1 = \frac{\mathbf{G}_1}{\|\mathbf{G}_1\|}$, $\mathbf{t}_2 = \frac{\mathbf{G}_3 \times \mathbf{G}_1}{\|\mathbf{G}_3 \times \mathbf{G}_1\|}$, $\mathbf{t}_2 = \mathbf{t}_1 \times \mathbf{t}_2$, the transformation to the local orthonormal basis system \mathbf{t}_i is given as $\mathbf{E} = \mathbf{T}_s^{-1} \mathbf{E}_{cova}$

The covariant components of the electric field are also arranged in a vector $\vec{\mathbf{E}}_{cova} = [\vec{E}_1, \vec{E}_2, \vec{E}_3]^T$ with

$$\vec{E}_i = -\frac{\partial \varphi}{\partial \xi^i} \quad (4)$$

where φ denotes the electric potential. With the Jacobian matrix

$$\mathbf{J} = \begin{bmatrix} J_{11} & J_{12} & J_{13} \\ J_{21} & J_{22} & J_{23} \\ J_{31} & J_{32} & J_{33} \end{bmatrix} \quad (5)$$

the transformation to the local orthonormal basis system is determined by $\vec{\mathbf{E}} = \mathbf{J}^{-1} \vec{\mathbf{E}}_{cova}$

The strains and the electric field are arranged in the vector

$$\boldsymbol{\varepsilon} = \begin{bmatrix} \mathbf{E} \\ \vec{\mathbf{E}} \end{bmatrix} \quad (6)$$

3. Constitutive equations

The relation between stresses, dielectric displacements, strains, and the electric field is assumed to be:

$$\boldsymbol{\sigma} = \mathbb{D} \boldsymbol{\varepsilon} \quad (7)$$

In Eq. (7) the vector $\boldsymbol{\sigma}$ is defined as $\boldsymbol{\sigma} = [\mathbf{S}, -\vec{\mathbf{D}}]^T$, where \mathbf{S} is the stress vector and $\vec{\mathbf{D}}$ the vector of dielectric displacements. The constant material matrix \mathbb{D} is given as:

$$\mathbb{D} = \begin{bmatrix} \mathbb{C} & -\mathbf{e} \\ -\mathbf{e}^T & -\boldsymbol{\epsilon} \end{bmatrix} \quad (8)$$

where \mathbb{C} is the elasticity matrix, \mathbf{e} is the piezoelectric matrix and $\boldsymbol{\epsilon}$ the permittivity matrix. The stored energy function is defined as:

$$W_0 = \frac{1}{2} \boldsymbol{\varepsilon}^T \mathbb{D} \boldsymbol{\varepsilon} \quad (9)$$

4. Variational formulation

In this section a variational functional of the Hu–Washizu type with six independent fields is introduced as:

$$\begin{aligned} \Pi(\mathbf{u}, \varphi, \bar{\boldsymbol{\varepsilon}}, \tilde{\boldsymbol{\sigma}}) = & \int_{B_0} W_0(\bar{\boldsymbol{\varepsilon}}) - \tilde{\boldsymbol{\sigma}} \cdot (\bar{\boldsymbol{\varepsilon}} - \boldsymbol{\varepsilon}) \, dV \\ & - \int_{B_0} \mathbf{b} \cdot \mathbf{u} \, dV - \int_{\partial_t B_0} \mathbf{t} \cdot \mathbf{u} \, dA \\ & + \int_{\partial_q B_0} q \varphi \, dA \end{aligned} \quad (10)$$

where:

$$\tilde{\boldsymbol{\sigma}} = \begin{bmatrix} \tilde{\mathbf{S}} \\ -\tilde{\vec{\mathbf{D}}} \end{bmatrix}, \quad \bar{\boldsymbol{\varepsilon}} = \begin{bmatrix} \bar{\mathbf{E}} \\ \bar{\vec{\mathbf{E}}} \end{bmatrix} \quad (11)$$

are functions of the independent quantities $\tilde{\mathbf{S}}$, $\tilde{\vec{\mathbf{D}}}$, $\bar{\mathbf{E}}$, and $\bar{\vec{\mathbf{E}}}$. The body force \mathbf{b} is defined in the reference configuration \mathcal{B}_0 and \mathbf{t} is the prescribed traction vector on the boundary $\partial_t \mathcal{B}_0$. The electric surface charge q is prescribed on the boundary $\partial_q \mathcal{B}_0$. Let $\mathcal{U} := \{\delta \mathbf{u} \in [H^1(\mathcal{B}_0)]^3 \mid \delta \mathbf{u}|_{\partial_t \mathcal{B}_0} = 0\}$ be the space of admissible displacement variations and $\mathcal{V} := \{\delta \varphi \in [H^1(\mathcal{B}_0)]^3 \mid \delta \varphi|_{\partial_q \mathcal{B}_0} = 0\}$ be the space of admissible electric potential variations. Further let $\tilde{\mathcal{S}} = \bar{\boldsymbol{\varepsilon}} = [L_2(\mathcal{B}_0)]$ be the spaces of admissible variations of the variables $\bar{\boldsymbol{\varepsilon}}$, $\tilde{\boldsymbol{\sigma}}$. The first variation reads:

$$\begin{aligned}
\delta \Pi &= \int_{B_0} \delta \bar{\boldsymbol{\varepsilon}} \cdot \left(\frac{\partial W_0}{\partial \bar{\boldsymbol{\varepsilon}}} - \tilde{\boldsymbol{\sigma}} \right) dV + \int_{B_0} \delta \tilde{\boldsymbol{\sigma}} \cdot (\boldsymbol{\varepsilon} - \bar{\boldsymbol{\varepsilon}}) dV \\
&+ \int_{B_0} \delta \boldsymbol{\varepsilon} \cdot \tilde{\boldsymbol{\sigma}} - \delta \mathbf{u} \cdot \mathbf{b} dV \\
&- \int_{\partial_t B_0} \delta \mathbf{u} \cdot \mathbf{t} dA + \int_{\partial_q B_0} \delta \varphi q dA = 0
\end{aligned} \quad (12)$$

The variation of the strains and the electric field result in

$$\delta E_{ij} = \frac{1}{2} \left(\frac{\delta u_i}{\xi^i} \cdot \mathbf{g}_j + \mathbf{g}_i \cdot \frac{\delta u_j}{\xi^j} \right), \quad \delta \bar{E}_i = \frac{\delta \varphi}{\xi^i} \quad (13)$$

The weak form is solved iteratively within the finite element method by employing Newton–Raphson’s method. This requires the linearization of Eq. (12), which reads:

$$\begin{aligned}
D[\delta \Pi] \cdot (\Delta \mathbf{u}, \Delta \varphi, \Delta \bar{\boldsymbol{\varepsilon}}, \Delta \tilde{\boldsymbol{\sigma}}) &= \int_{B_0} \delta \bar{\boldsymbol{\varepsilon}} \cdot \frac{\partial \partial W_0}{\partial \bar{\boldsymbol{\varepsilon}} \partial \bar{\boldsymbol{\varepsilon}}} \Delta \bar{\boldsymbol{\varepsilon}} \\
&- \delta \bar{\boldsymbol{\varepsilon}} \cdot \Delta \tilde{\boldsymbol{\sigma}} dV \\
&+ \int_{B_0} \delta \tilde{\boldsymbol{\sigma}} \cdot \Delta \boldsymbol{\varepsilon} - \delta \tilde{\boldsymbol{\sigma}} \cdot \Delta \bar{\boldsymbol{\varepsilon}} dV \\
&+ \int_{B_0} \delta \boldsymbol{\varepsilon} \cdot \Delta \tilde{\boldsymbol{\sigma}} + \tilde{\boldsymbol{\sigma}} \cdot \Delta \delta \boldsymbol{\varepsilon} dV
\end{aligned} \quad (14)$$

$$\text{with } \Delta \delta \boldsymbol{\varepsilon} = [\Delta \delta \mathbf{E}^T, 0]^T \text{ and } \Delta \delta E_{ij} = \frac{1}{2} \left(\frac{\delta u_i}{\xi^i} \cdot \frac{\delta u_j}{\xi^j} + \frac{\delta u_j}{\xi^j} \cdot \frac{\delta u_i}{\xi^i} \right)$$

5. Finite element approximations

The finite element approximation is constructed in the sense that the whole domain is divided in element domains with $\mathcal{B} = \cup_{e=1}^{nelm} \mathcal{B}_e$, where *nelm* is the total number of elements. The geometry, displacements and electric potential are approximated as:

$$\mathbf{X}_e^h = \sum_{I=1}^8 N_I \mathbf{X}_I, \quad \mathbf{u}_e^h = \sum_{I=1}^8 N_I \mathbf{u}_I, \quad \varphi_e^h = \sum_{I=1}^8 N_I \varphi_I \quad (15)$$

with the same interpolation function

$$N_I = \frac{1}{8} (1 + \xi_I^1 \xi^1) (1 + \xi_I^2 \xi^2) (1 + \xi_I^3 \xi^3), \quad -1 \leq \xi^i \leq +1 \quad (16)$$

at the node $I = 1, 2, 3, \dots, 8$. The vectors \mathbf{X}_I , \mathbf{u}_I contain the nodal co-ordinates and the nodal displacements, respectively. Arranging N_I in the matrix $\mathbf{N} = [N_1, N_2, N_3, N_4, N_5, N_6, N_7, N_8]$ with $N_I = \text{diag}[N_I, N_I, N_I, N_I]$, the virtual displacements and the electric potential are interpolated as:

$$\begin{bmatrix} \delta \mathbf{u}_e^h \\ \delta \varphi_e^h \end{bmatrix} = \mathbf{N} \delta \mathbf{v}_e \quad (17)$$

where $\mathbf{v}_e^T = [\mathbf{v}_1^T, \mathbf{v}_2^T, \mathbf{v}_3^T, \dots, \mathbf{v}_8^T]$ is the nodal vector with $\mathbf{v}_1^T = [u_1, u_2, u_3, \varphi]_1^T$

The approximation of the virtual gradient field $\boldsymbol{\varepsilon}$ reads

$$\delta \boldsymbol{\varepsilon}_e^h = \mathbf{B} \delta \mathbf{v}_e \quad (18)$$

with $\mathbf{B} = [\mathbf{B}_1, \mathbf{B}_2, \mathbf{B}_3, \mathbf{B}_4, \mathbf{B}_5, \mathbf{B}_6, \mathbf{B}_7, \mathbf{B}_8]$ and

$$\mathbf{B}_I = \begin{bmatrix} \mathbf{B}_I^u & \mathbf{0} \\ \mathbf{0} & \mathbf{B}_I^\phi \end{bmatrix}$$

The matrix \mathbf{B}_I^u is defined in [6] by employing some assumed natural strain interpolations. The matrix \mathbf{B}_I^ϕ at the node I is given as:

$$\mathbf{B}_I^\phi = \mathbf{J}^{-1} \begin{bmatrix} N_{I,\xi^1} \\ N_{I,\xi^2} \\ N_{I,\xi^3} \end{bmatrix} \quad (19)$$

In the linearized weak form Eq. (14) the quantity $\Delta \delta \mathbf{E} : \tilde{\mathbf{S}}$ appears, which is approximated as:

$$(\Delta \delta \mathbf{E} : \tilde{\mathbf{S}})^h = \delta \mathbf{v}_e^T \mathbf{G} \Delta \mathbf{v}_e \quad (20)$$

where the matrix \mathbf{G} is also given in [6].

The independent field $\bar{\boldsymbol{\varepsilon}}$ is approximated with the following interpolation:

$$\begin{aligned}
\bar{\boldsymbol{\varepsilon}}_e^h &= \mathbf{M}_\alpha \boldsymbol{\alpha} \quad \text{with} \quad \mathbf{M}_\alpha = \begin{bmatrix} N_E & \mathbf{M}_E & \mathbf{0} & \mathbf{0} \\ \mathbf{0} & \mathbf{0} & N_{\bar{E}} & \mathbf{M}_{\bar{E}} \end{bmatrix} \\
&\text{and } \boldsymbol{\alpha} \in \mathbb{R}^{40}
\end{aligned} \quad (21)$$

The matrices N_E , \mathbf{M}_E are given in [6], whereas the matrices $N_{\bar{E}}$, $\mathbf{M}_{\bar{E}}$ are defined as:

$$N_{\bar{E}} = \mathbf{J}_0^T \begin{bmatrix} 1 & 0 & 0 & \xi^2 & \xi^3 & \xi^2 \xi^3 & 0 & 0 & 0 & 0 & 0 & 0 \\ 0 & 1 & 0 & 0 & 0 & 0 & \xi^1 & \xi^3 & \xi^1 \xi^3 & 0 & 0 & 0 \\ 0 & 0 & 1 & 0 & 0 & 0 & 0 & 0 & 0 & \xi^1 & \xi^2 & \xi^1 \xi^2 \end{bmatrix} \quad (22)$$

$$\mathbf{M}_{\bar{E}} = \frac{\det \mathbf{J}_0}{\det \mathbf{J}} \mathbf{J}_0^{-1} \begin{bmatrix} 0 & 0 & 0 \\ 0 & 0 & 0 \\ \xi^3 & \xi^1 \xi^3 & \xi^2 \xi^3 \end{bmatrix} \quad (23)$$

The Jacobian with the index 0 is evaluated at the element center. According to Eq. (23) the approximation of the electric field $\hat{\mathbf{E}}$ is a bi-linear function through the thickness. The approximation of the independent field $\bar{\boldsymbol{\varepsilon}}$ is defined as:

$$\bar{\boldsymbol{\varepsilon}}_e^h = \mathbf{M}_\beta \boldsymbol{\beta} \quad \text{with} \quad \mathbf{M}_\beta = \begin{bmatrix} N_S & \mathbf{0} \\ \mathbf{0} & N_{\bar{E}} \end{bmatrix} \quad \text{and} \quad \boldsymbol{\beta} \in \mathbb{R}^{30} \quad (24)$$

For the matrix N_S see [6]. Considering the above interpolations in Eqs. (12) and (14) one obtains the following matrices:

$$A_e = \int_{B_e} \mathbf{M}_\alpha^T \mathbb{D} \mathbf{M}_\alpha dV_e \quad C_e = \int_{B_e} \mathbf{M}_\alpha^T \mathbf{M}_\beta \quad (25)$$

$$L_e = \int_{B_e} \mathbf{B}^T \mathbf{M}_\beta dV_e \quad K_e = \int_{B_e} \mathbf{G} dV_e$$

and vectors

$$\begin{aligned} \mathbf{a}_e &= \int_{B_e} \mathbf{M}_\alpha^T (\boldsymbol{\sigma} - \tilde{\boldsymbol{\sigma}}) dV_e & \mathbf{b}_e &= \int_{B_e} \mathbf{M}_\beta^T (\boldsymbol{\varepsilon} - \bar{\boldsymbol{\varepsilon}}) dV_e \\ \mathbf{f}_e^{int} &= \int_{B_e} \mathbf{B}^T \tilde{\boldsymbol{\sigma}} dV_e & \mathbf{f}_e^{ext} &= \int_{B_e} \mathbf{N}^T \tilde{\mathbf{p}} dV_e \\ & & &+ \int_{\partial B_e} \mathbf{N}^T \tilde{\mathbf{t}} dA_e \end{aligned} \quad (26)$$

In Eq. (26) the body and surface loads are determined by $\tilde{\mathbf{p}}^T = [\mathbf{b}^T, 0]$ and $\tilde{\mathbf{t}}^T = [\mathbf{t}^T, q]$. With respect that Eq. (12) is solved iteratively with Newton's method, the following approximation on element level is obtained:

$$\begin{aligned} &[\delta \Pi + \mathbf{D}[\delta \Pi] \cdot (\Delta \mathbf{u}, \Delta \phi, \Delta \bar{\boldsymbol{\varepsilon}}, \Delta \tilde{\boldsymbol{\sigma}})]_e^h \Rightarrow \\ &\begin{bmatrix} \delta v_e \\ \delta \boldsymbol{\alpha}_e \\ \delta \boldsymbol{\beta}_e \end{bmatrix}^T \left(\begin{bmatrix} \mathbf{f}_e^{int} - \mathbf{f}_e^{ext} \\ \mathbf{a}_e \\ \mathbf{b}_e \end{bmatrix} + \begin{bmatrix} K_e & \mathbf{0} & L_e \\ \mathbf{0} & A_e & -C_e \\ L_e^T & -C_e^T & \mathbf{0} \end{bmatrix} \begin{bmatrix} \Delta v_e \\ \Delta \boldsymbol{\alpha}_e \\ \Delta \boldsymbol{\beta}_e \end{bmatrix} \right) \end{aligned} \quad (27)$$

Taking into account that the finite element interpolations for the fields $\bar{\boldsymbol{\varepsilon}}$, $\tilde{\boldsymbol{\sigma}}$ are discontinuous across the element boundaries, a condensation on element level yields the element stiffness matrix and the right-hand side:

$$K_{Te} = K_e + L_e (C_e^T A_e^{-1} C_e)^{-1} L_e^T$$

$$\mathbf{f}_e = \mathbf{f}_e^{ext} - \mathbf{f}_e^{int} - L_e (C_e^T A_e^{-1} C_e)^{-1} (C_e^T A_e^{-1} \mathbf{a}_e + \mathbf{b}_e) \quad (28)$$

After assembly over all elements $\mathbf{K}_T = A_{e=1}^{nelm} K_{Te}$, $\Delta \mathbf{V} = A_{e=1}^{nelm} \Delta v_e$ and $\mathbf{P} = A_{e=1}^{nelm} \mathbf{f}_e$ one obtains

$$\mathbf{K}_T \Delta \mathbf{V} = \mathbf{P} \quad (29)$$

with the unknown incremental nodal displacements and the electric potential. The update of the internal degrees of freedoms reads

$$\begin{aligned} \Delta \boldsymbol{\beta}_e &= (C_e^T A_e^{-1} C_e)^{-1} (L_e^T \Delta v_e + C_e^T A_e^{-1} \mathbf{a}_e + \mathbf{b}_e) \\ \Delta \boldsymbol{\alpha}_e &= A_e^{-1} (C_e \Delta \boldsymbol{\beta}_e - \mathbf{a}_e) \end{aligned} \quad (30)$$

6. Numerical example

In this example the buckling behavior of a piezoelectric plate loaded by an electric field is analyzed. A square plate consisting of six layers is considered; the layup and the geometry data of the plate are given in Fig. 1. The principal directions of the graphite epoxy plies lie in the X_1 - X_2 plane. Here the angle is introduced with respect to the X_1 axis.

The elastic material data for graphite epoxy is determined by the Young's moduli $E_1 = 132.4$ GPa, $E_2 = E_3 = 10.8$ GPa, Poisson ratios $\nu_{12} = \nu_{13} = 0.24$, $\nu_{23} = 0.49$ and the shear moduli $G_{12} = G_{13} = 5.6$ GPa, $G_{23} = 3.6$ GPa. According to [5] PZT 5 is characterized with respect to the co-ordinate system given in Fig. 1 by the

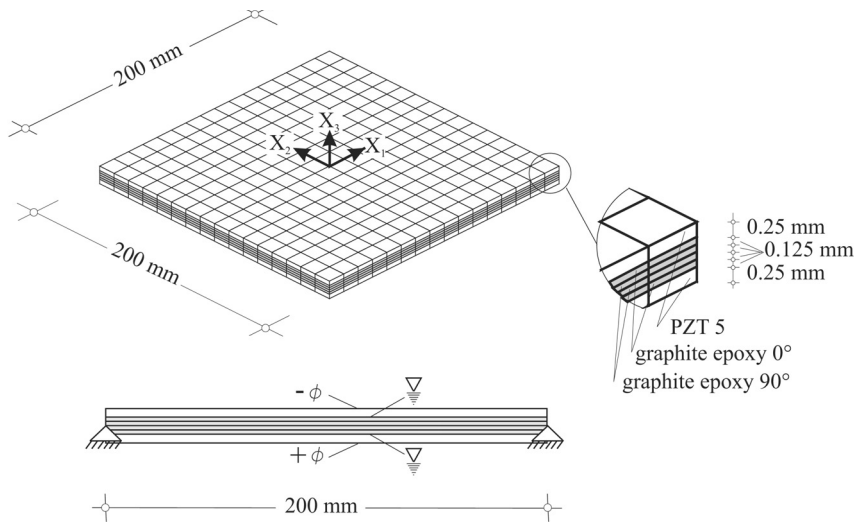


Fig. 1. Finite element model of the laminated square plate with loading and boundary conditions.

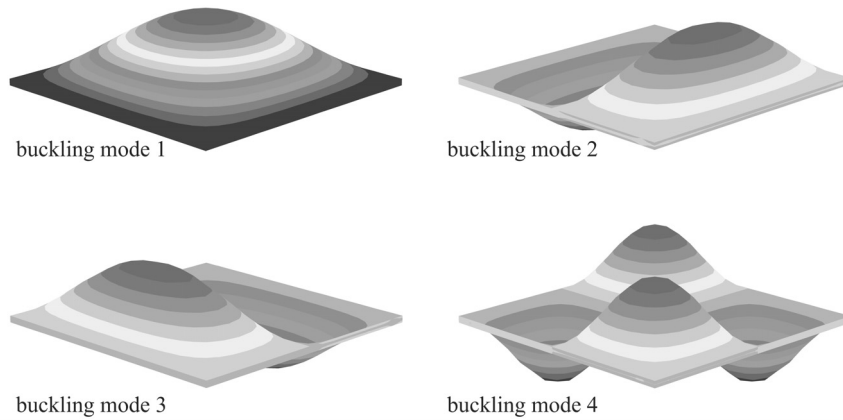


Fig. 2. First four piezoelectric buckling modes with a plot of the normalized u_3 displacement.

elasticity constants $E_1 = E_2 = 62$ GPa, $E_3 = 54$ GPa, $\nu_{12} = \nu_{13} = \nu_{23} = 0.31$, $G_{12} = G_{13} = 23.6$ GPa, $G_{23} = 18$ GPa; by the piezoelectric coefficients $d_{31} = d_{32} = -220$ pm/V, $d_{33} = 440$ pm/V, $d_{25} = d_{16} = 670$ pm/V; and by the electric permittivity $\epsilon_{11} = \epsilon_{22} = \epsilon_{33} = 22.9923$ nF/m, where the values E_3, d_{33} are assumed.

Plate buckling based on piezoelectric effects is observed by increasing the electric potential φ up to a critical value. The first four buckling modes are calculated and shown in Fig. 2. The corresponding critical values of φ are listed in Table 1. The good agreement with [5] of the critical electric potentials calculated with the present element is noted.

Table 1.
Critical electric potential φ [V] for the first four buckling modes

Order	Present solid shell element	Reference [5]
1	70.58	68.8
2	172.47	170.5
3	193.26	189.4
4	286.07	289.3

One possible application of the described buckling behavior could be a switch device. In addition to [5] we introduce such a device, in which the geometry of the considered plate is slightly modified by reducing the thickness of the upper piezoelectric layer to 0.249 mm. This geometrical imperfection initializes the buckling direction, thus the stability problem becomes a pure bending problem. In Fig. 3 the electric potential φ is plotted versus the vertical deflection at the center point of the plate. An increasing load from $\varphi = 60$ V to $\varphi = 120$ V leads to a large change in the displacement

response $u_3 = 0.002$ mm to $u_3 = 0.731$ mm. This effect may be utilized for a switching device.

7. Conclusion

In this paper a geometrically nonlinear solid shell element to analyze piezoelectric structures is presented. The mixed formulation fulfills the electric charge conservation law exactly. A numerical example demonstrates the applicability to piezoelectric buckling problems.

References

- [1] Kögel M, Bucalem ML. Locking-free piezoelectric MITC shell elements. In: KJ Bathe, editor, Computational Fluid and Solid Mechanics. Oxford: Elsevier 2003.
- [2] Bernadou M, Haenel C. Modelization and numerical approximation of piezoelectric thin shells; Part II: Approximation by finite element methods and numerical experiments. *Comp Meth Appl Mech Eng* 2003;192:4045–4073.
- [3] Sze KY, Yao LQ, Yi S. A hybrid stress ANS solid-shell element and its generalization for smart structure modelling; Part II: Smart structure modelling. *Int J Num Meth Eng* 2000;48:565–582.
- [4] Tzou HS, Zhou YH. Nonlinear piezothermoelasticity and multi-field actuations; Part 2: Control of nonlinear deflection, buckling, and dynamics. *J Vibr Acoustics* 1997;119:382–389.
- [5] Varelis D, Saravanos DA. Nonlinear coupled mechanics and initial buckling of composite plates with piezoelectric actuators and sensors. *Smart Mater Struct* 2002;11:330–336.

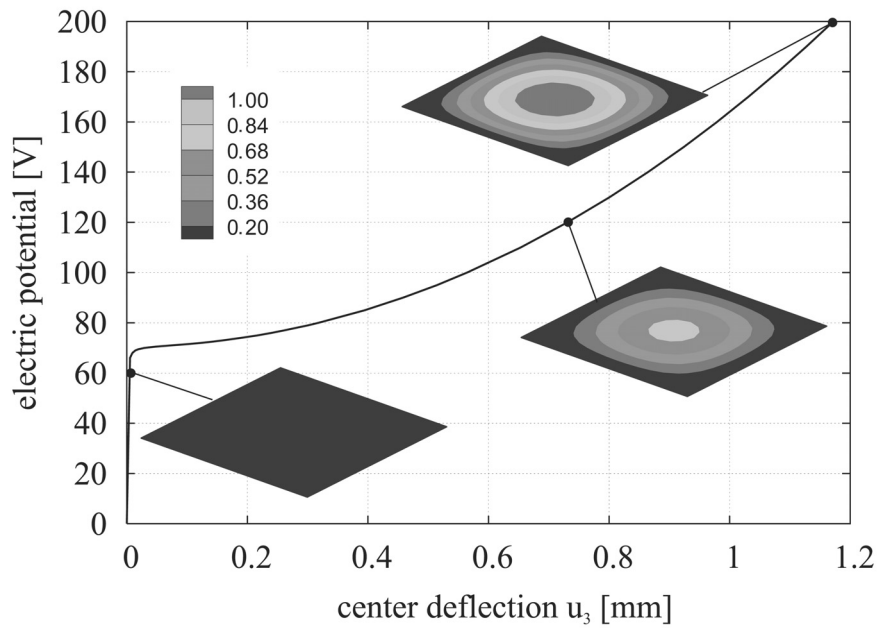


Fig. 3. Load deflection curve and plots of the vertical deflection at characteristic points.

[6] Klinkel S, Gruttmann F, Wagner W. Four-field mixed formulation for a solid shell element. In: ZH Yao, MW

Yuan, WX Zhong, editors, Computational Mechanics Proc. WCCM IV, 2004.